

Multi-view Graph Contrastive Representation Learning for Drug-Drug Interaction Prediction

Yingheng Wang¹, Yaosen Min², Xin Chen³, Ji Wu¹

¹Department of Electronic Engineering, Tsinghua University

²Institute of Interdisciplinary Information Sciences, Tsinghua University

³Technology and Engineering Group, Tencent

¹wangyh20@mails.tsinghua.edu.cn, wuji_ee@mail.tsinghua.edu.cn

²minys18@mails.tsinghua.edu.cn

³marcuschen@tencent.com

ABSTRACT

Potential Drug-Drug Interaction (DDI) occurring while treating complex or co-existing diseases with drug combinations may cause changes in drugs' pharmacological activity. Therefore, DDI prediction has been an important task in the medical healthy machine learning community. Graph-based learning methods have recently aroused widespread interest and are proved to be a priority for this task. However, these methods are often limited to exploiting the inter-view drug molecular structure and ignoring the drug's intra-view interaction relationship, vital to capturing the complex DDI patterns. This study presents a new method, multi-view graph contrastive representation learning for drug-drug interaction prediction, MIRACLE for brevity, to capture inter-view molecule structure and intra-view interactions between molecules simultaneously. MIRACLE treats a DDI network as a multi-view graph where each node in the interaction graph itself is a drug molecular graph instance. We use GCN to encode DDI relationships and a bond-aware attentive message propagating method to capture drug molecular structure information in the MIRACLE learning stage. Also, we propose a novel unsupervised contrastive learning component to balance and integrate the multi-view information. Comprehensive experiments on multiple real datasets show that MIRACLE outperforms the state-of-the-art DDI prediction models consistently.

CCS CONCEPTS

• **Mathematics of computing** → **Graph algorithms**; • **Applied computing** → **Health informatics**; • **Computing methodologies** → **Supervised learning by classification**.

KEYWORDS

multi-view graph, contrastive learning, link prediction, graph embedding

1 INTRODUCTION

Drugs may interact with each other when drug combinations occur, which will alter their effects. Such situations can increase the risk of patients' death or drug withdrawal, particularly in the elderly, with a prevalence of 20-40%[32]. Recent studies estimate that 6.7% of the US hospitalized patients have a severe adverse drug reaction with a fatality rate of 0.32%[21]. However, polypharmacy is inevitable because the concurrent use of multiple medications is necessary for treating diseases that are often caused by complex biological

processes that resist the activity of any single drug. Hence, there is a practical necessity to identify the interaction of drugs.

Detection of DDI remains a challenging task: traditional wet chemical experiments are expensive and cumbersome, and too small in scale, limiting the efficiency of DDIs detection. Besides, there are tedious and time-consuming clinical tests and patient follow-up afterward. These problems make it urgent to develop a new, computationally assisted DDI prediction method.

The machine learning methods facilitate the computer-assisted DDI prediction. Prior approaches to DDI prediction focused mainly on inputting various fingerprints or similarity-based features such as [46]. In the early years, research works like [45] are designed very simple and only considering a single fingerprint. After 2014, plenty of research works based on multi-source heterogeneous fingerprints flourished. Kastrin et al. [15] establishes a logistic regression model with similarity-based features constructed on side effects and physiological effects between a pair of drugs as inputs. Using features such as the multi-dimensional molecular structures, individual drug side effects, and interaction profile fingerprints, Ryu et al. [36] use various deep learning-based methods to integrate different types of inputs by learning latent representations and find DDI.

In recent years, many graph representation learning-based methods have been applied to extracting features from raw molecular graph data. Zitnik et al. [57] constructs a heterogeneous network including drug and protein entities and uses graph convolutional network (GCN)[18] to learn latent representations, then predicts possible adverse effect types occurring in drug combinations. Ma et al. [27] proposes a method integrating multi-view similarity-based features by attention mechanism, where a view refers to a similarity matrix constructed by a feature and learns drug representations with graph autoencoder (GAE)[19]. Deac et al. [4] applies a co-attention mechanism to compute the attentional coefficients between all atoms in a pair of drugs to learn joint drug-drug information better. Chen et al. [3] uses a siamese GCN to learn the pairwise drug representations and make predictions with a similarity-based method.

Although the methods above achieve satisfactory results and become the state-of-the-art, they still have some limitations. *Firstly*, previous models based on multiple similarity-based fingerprints require feature engineering or integration of these drug features, which are time-consuming and challenging to collect[48]. They mainly rely on the empirical assumption that chemically, biologically, or topologically similar drugs are more likely to interact with

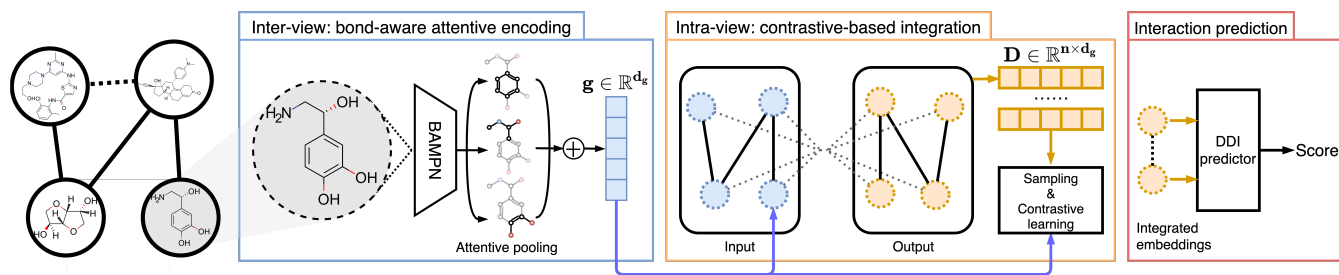


Figure 1: The illustrative schematic diagram of our proposed framework MIRACLE. There are three sequential and interdependent phases: 1) In the inter-view, drug molecular graphs are encoded into drug embeddings by a bond-aware message passing network with attentive pooling. 2) In the intra-view, a GCN encoder is used to integrate the external DDI relationships into drug embeddings. Also, a contrastive learning-based method is applied to balance information from different views to update drug embeddings. 3) With the learned drug embeddings, an interaction predictor is designed to generate final prediction results.

each other. However, plenty of interacting drug pairs whose pairwise similarities are extremely low may be led to wrong prediction results. Meanwhile, large-scale datasets may be missing some of these features, which are crucial to DDI prediction but unavailable for most kinds of drugs. Therefore, these models **have a deficiency in the scalability and robustness**. *Secondly*, in practice, the inter-view information included in the drug molecular graph and the intra-view DDI relationships are important for the DDI prediction task. The inter-view information contains multiple atom and bond’s features and structure information inside drug molecules. Besides, the interaction patterns are hidden in the intra-view DDI relationships. However, previous graph-based works only concentrate on a single view of drugs[48]. Thus, **the combination of multi-views information inside the DDI network is often overlooked** by these methods.

To overcome the limitations mentioned above, we proposed a novel method, Multi-view gRAph Contrastive representation Learning for drug-drug interaction prediction, MIRACLE for brevity, to explore rich multi-views information among drugs and generate accurate latent vectors of drugs. In such a multi-view graph setting, we treat each drug instance as a molecular graph and DDI relationships as an interaction graph, namely the inter- and intra-view, respectively. In the inter-view, we first encode drug molecular graphs into drug embeddings by a bond-aware message passing network fusing information from atom and bond features and molecule structures. Then, we integrate them with the intra-view information, the external DDI relationships to update drug embedding. Also, for the multi-view information integrated into drug embeddings, it is necessary to balance information from different views. We use a contrastive learning-based method to tackle this problem. To supplement structural information in drug embedding for the final interaction prediction, we apply an algorithm to encode interaction-wise substructures and make predictions based on an ensemble of it and drug embedding.

Figure 1 illustrates the framework of the proposed MIRACLE method. At first, all drug instances are modeled as molecular graphs, where each node represents an atom, and each edge is a bond. Then,

each molecular graph is proceeded successively. The inter-view latent vectors for all drugs involved in the DDI network can be obtained through a bond-aware message passing neural networks with attentive pooling. After that, we integrate the inter-view and intra-view information to update drug representations by a GCN encoder where we treat drug instances as nodes, the inter-view drug embeddings as node features, and the external DDI relationships as graph connectivity. For balancing information from different views better, we design a novel contrastive learning component to optimize the model by setting a mutual information maximization objective. We also apply a double-radius node label(DRNL) algorithm to encode the interaction-wise substructure information to aid predictions. Finally, we use a two-layer fully-connected neural network to make predictions with the obtained drug embeddings and encoded substructure information. To help MIRACLE learn the commonality between two views well, we also make predictions using the inter-view drug representations and define a disagreement loss to enforce prediction results in two views to a consistency. The main contributions of this work are summarized as follows:

- We model the DDI data in a multi-view graph setting and use graph representation learning methods to capture complex interaction patterns. To the best of our knowledge, it is a brand new perspective and has not been studied before.
- To balance multiple views information in the drug representations, we do not rely on the supervised information only but design a novel contrastive learning component to update drug embeddings by a mutual information maximization objective.
- Extensive experiments conducted on a variety of real-world datasets show that MIRACLE evidently outperforms the state-of-art methods by a large margin, even when given very few labeled training instances.

2 METHODOLOGY

This section introduces the proposed DDI prediction approach, which is an end-to-end representation learning model consisting

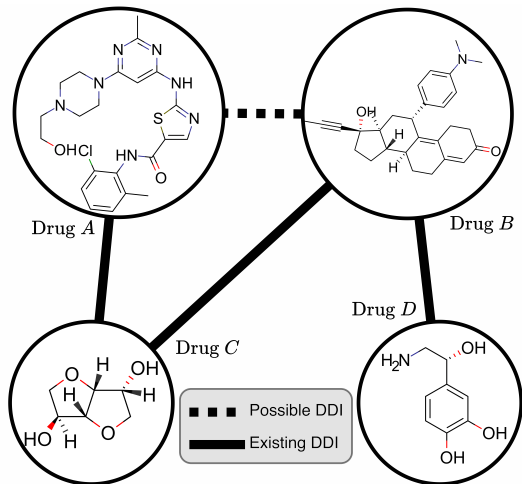


Figure 2: A toy example of the multi-view graph.

of three sequential and interdependent phases. At first, we define a bond-aware message passing network with attentive pooling, which encodes drug molecular graph data to corresponding low-dimensional embedding vectors. The second is an information integration module that uses a GCN to integrate the drug molecule corresponding to low-dimensional embedding vectors with the external DDI relationships. The Last is an interaction predictor, which is responsible for predicting missing interactions in a DDI Network.

Figure 2 shows a multi-view graph in the context of a DDI network. Drug A, B, C, D denote four drugs in the DDI network. The solid and dashed lines indicate existing and possible interactions. The internal structure of each drug shows its molecular graph.

The proposed model takes the SMILES representation of the corresponding drug molecule and the DDI network connectivity matrix as inputs. The SMILES representation will be converted into a molecular graph via RDKit[20]. Meanwhile, we extract the atom list and multi-channel adjacency matrix from the molecular graph, which will be fed into the following bond-aware message passing network. In this section, we will depict the architecture, optimization objective, and training process.

2.1 Notations and Problem Formulation

Before presenting our proposed model, We summarize the important notations adopted in this paper. We use upper boldface letters for matrices (e.g. $\mathbf{A} \in \mathbb{R}^{m \times n}$), boldface letters for vectors (e.g. $\mathbf{h} \in \mathbb{R}^d$), normal characters for scalars (e.g. d_g for the dimension of molecule-level embedding, d_h for the dimension of atom-level embedding), and calligraphic for sets (e.g. \mathcal{G}).

Suppose that we have a graph \mathcal{G} which is presented by $\mathcal{G} = \{\mathcal{V}, \mathcal{E}\}$ where \mathcal{V} is the set of vertices and \mathcal{E} is the set of edges. We denote the i th atom as $v_i \in \mathcal{V}$ and the chemical bond connecting the i th and j th atoms as $e_{ij} \in \mathcal{E}$.

Problem statement. The DDI prediction task can be defined as a link prediction problem on graph. Given g drug molecular graphs $\mathcal{G} := \{\mathcal{G}^{(i)}\}_{i=1}^g$ and DDI network $\mathcal{N} = (\mathcal{G}, \mathcal{L})$ where \mathcal{L} denotes

the interaction links, the task link prediction is, for the network \mathcal{N} , predicting the existence of missing links.

2.2 Bond-aware Message Passing Network with Attentive Pooling

Since the molecular graphs are complex irregular-structured data to handle, in this subsection, we use a bond-aware Message Passing Network[8](MPN) to map nodes to real-valued embedding vectors in the low-dimensional space. We equipped our model with propagation-based message passing layers according to simple chemistry knowledge and a graph aggregation layer with attentive pooling[42] to generate a graph-level representation.

A molecule can be abstracted as a graph where each atom is represented as a node and each bond as an edge. We construct the node information matrix by stacking randomly-initialized embedding vectors for each atom considering its nuclear charge number and a multi-channel adjacency matrix whose channel dimension indicates different chemical types, including single double, triple and aromatic bond.

Given the node information matrix and multi-channel adjacency matrix as inputs, we encode them by two successive processes of Message Passing. The first phase can be described using the following message function:

$$\tilde{\mathbf{h}}_i^{(l)} = \sum_{j \in C(i)} \mathbf{W}_{c_{ij}}^{(l)} \mathbf{h}_j^{(l-1)} \quad (1)$$

where $\mathbf{W}_{c_{ij}}^{(l)} \in \mathbb{R}^{d_h \times d_h}$ is a matrix of trainable parameters shared by the same type of chemical bond e_{ij} at the l th layer, $\tilde{\mathbf{h}}_i^{(l)}$ represents the candidate hidden state at the l th layer for node v_i , $\mathbf{h}_j^{(l-1)} \in \mathbb{R}^{d_h}$ represents the hidden state at the $(l-1)$ th layer for the neighbor node v_j , and $C(i)$ denotes the neighbor nodes of the center node v_i .

The equation(1) shows that the node information corresponding to the same type of chemical bond share parameters during the affine transformation. The chemical interpretability for this message function is straightforward: neighboring nodes connected by the same type of chemical bond have similar effects, and vice versa.

Given $\hat{\mathbf{h}}_i^{(l)} = [\mathbf{h}_i^{(l-1)}; \tilde{\mathbf{h}}_i^{(l)}]$ where $[\cdot; \cdot]$ denotes the concatenation operation, for the second phase, inspired by [39], we additionally define three non-linear transforms $F(\mathbf{W}_f, \hat{\mathbf{h}}_i^{(l)})$, $T(\mathbf{W}_t, \hat{\mathbf{h}}_i^{(l)})$, and $C(\mathbf{W}_c, \hat{\mathbf{h}}_i^{(l)})$. Thus, this process can be described as the following update function:

$$\mathbf{h}_i^{(l)} = T(\mathbf{W}_t, \hat{\mathbf{h}}_i^{(l)}) \odot F(\mathbf{W}_f, \hat{\mathbf{h}}_i^{(l)}) + C(\mathbf{W}_c, \hat{\mathbf{h}}_i^{(l)}) \odot \mathbf{h}_i^{(l-1)} \quad (2)$$

where $\mathbf{h}_i^{(l)}$ represents the hidden state at the l th layer for node v_i , and \odot denotes the element-wise product. We refer to F as the *fuse* gate, T as the *transform* gate, and C as the *carry* gate, since they express how much of the hidden state is produced by transforming the fusion of the candidate and previous hidden state and carrying it, respectively. We can take both the influence on the concentrated center node exerted by neighboring ones and itself at the previous layer into consideration through this update process.

We stack several message passing layers (L in total) to learn the hidden representation for every node/atom v in a molecular graph \mathcal{G}

and obtain the final hidden states for each atom at the last message passing layer. To make predictions with drug representations, we need to generate an embedding vector for each molecular graph. Therefore, we apply a simple but efficient attentive readout layer inspired by Li et al. [24] as follows:

$$\mathbf{a}_i = \tanh(\mathbf{W}_a[\mathbf{h}_i^{(0)}; \mathbf{h}_i^{(L)}] + \mathbf{b}_a) \quad (3)$$

$$\mathbf{g} = \sum_{v_i \in \mathcal{V}} \mathbf{a}_i \odot (\mathbf{W}_o \mathbf{h}_i^{(L)} + \mathbf{b}_o) \quad (4)$$

where $[\cdot]$ denotes the concatenation operation, $\tanh(\cdot)$ denotes the tanh activation function, attention score $\mathbf{a}_i \in \mathbb{R}^{d_g}$ denotes the importance score of the atom v_i , \odot denotes the hardamard product, and $\mathbf{g} \in \mathbb{R}^{d_g}$ is the obtained embedding vector for the molecular graph. Stacking the embedding vectors of drugs over given dataset, we get the inter-view embedding matrix $\mathbf{G} \in \mathbb{R}^{n \times d_g}$. It should be noted that all of the parameters are shared across all the atoms.

2.3 GCN for Integrating Multi-view Network Information

For drug molecular graphs, after the non-linear mapping introduced above, we get low-dimensional representations of them. In order to encode the intra-view interaction information into the drug embeddings, we establish an encoder to integrate the multi-view network information. Recently many representation learning based methods such as Kipf and Welling [18] have demonstrated their superiority to traditional methods such as various dimensionality reduction algorithms[51]. In this paper we make use of GCN in terms of efficiency and effectiveness. In the following, we utilized a multi-layer GCN(M in total) to smooth each node’s features over the graph’s topology. In this context, we refer to the node’s features as low-dimensional representations of drugs learned from the previous message passing network and the graph’s topology as the interaction relationship inside the DDI network.

Assumed the number of drugs in the DDI network is denoted by n , formally, we are given the adjacency matrix of DDI network $\mathbf{A} \in \mathbb{R}^{n \times n}$ and the attribute matrix $\mathbf{G} \in \mathbb{R}^{n \times d_g}$ of the DDI network \mathcal{N} as inputs. Before the graph convolution operation, we normalized the adjacency matrix \mathbf{A} :

$$\hat{\mathbf{A}} = \tilde{\mathbf{K}}^{-\frac{1}{2}} (\mathbf{A} + \mathbf{I}_n) \tilde{\mathbf{K}}^{-\frac{1}{2}} \quad (5)$$

where \mathbf{I}_n represents the identity matrix and $\tilde{\mathbf{K}}_{ii} = \sum_j (\mathbf{A} + \mathbf{I}_n)_{ij}$. Then we apply the GCN encoder framework as follows:

$$\mathbf{D}^{(1)} = U(\mathbf{A}, \mathbf{G}, \mathbf{W}_u^{(0)}, \mathbf{W}_u^{(1)}) = \hat{\mathbf{A}} \text{ReLU}(\hat{\mathbf{A}} \mathbf{G} \mathbf{W}_u^{(0)}) \mathbf{W}_u^{(1)} \quad (6)$$

where $\mathbf{W}_u^{(0)} \in \mathbb{R}^{d_u^{(0)} \times d_u^{(1)}}$ and $\mathbf{W}_u^{(1)} \in \mathbb{R}^{d_u^{(1)} \times d_u^{(2)}}$ are two weight parameters at the 0th and 1th layer of the GCN encoder, respectively. The second dimension of the weight parameter at the last layer of the GCN encoder is set to d_g . Through the GCN encoder, then we get the intra-view embedding matrix $\mathbf{D} \in \mathbb{R}^{n \times d_g}$ for drugs in the DDI network \mathcal{N} .

2.4 Contrastive Learning of Drug Representation

As stated in Li et al. [23], the graph convolution operation can be considered Laplacian smoothing for nodes’ features over graph

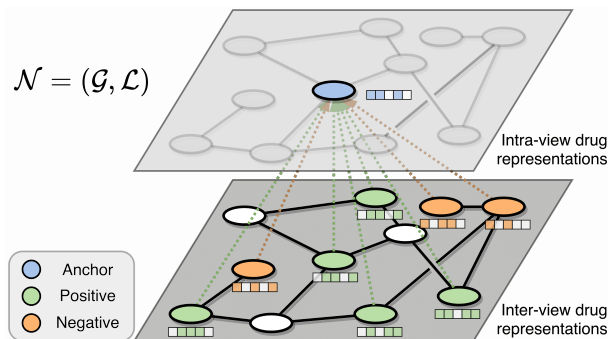


Figure 3: The proposed graph contrastive learning framework.

topology. The Laplacian smoothing computes the new node features as the weighted average of itself and its neighbors’. On the one hand, although it helps make nodes in the same cluster tend to learn similar representations, it may cause the over-smoothing problem and make nodes indistinguishable. On the other hand, it will concentrate so much on node features information that makes the learned embeddings lack structural information, which will be discussed and tackled in the next subsection.

Furthermore, the inter-view drug embeddings are learned directly from molecular graphs, including raw attributes and structural information. Specifically, the representations may contain multiple functional groups’ information inside a molecule, different local connectivity constructed by various combinations of the same atoms and bonds, etc. Such information has a significant influence on interaction predictions. However, after graph convolutions, the inter-view features are smoothed over the whole DDI network topology and become blurred. Therefore, it is necessary to balance multi-view information in the drug embeddings. In this subsection, we propose a novel graph contrastive learning framework to handle these issues.

Figure 3 illustrates the proposed graph contrastive learning component. In MIRACLE, we naturally have two different graph views in the multi-view graph setting to learn drug representations by maximizing the agreement between inter-view and intra-view embeddings. We define our mutual information(MI) estimator on inter- and intra-view pairs, maximizing the estimated MI over the given dataset \mathcal{N} . To be specific, for each drug i , fixing itself as an anchor A , we get a set of positive samples \mathbb{P} which is made up of itself and its k -order neighboring nodes, and a set of negative samples \mathbb{N} from nodes not in its k -hop neighbors. Considering the assumption that representations of drugs that interact with the same drug may contain similar information, we usually set $k = 2$. Then, we generate each positive pair (A, P) where $P \in \mathbb{P}$ and negative pair (A, N) where $N \in \mathbb{N}$. After iterations, we can obtain all possible positive pairs and negative pairs. Afterward, we employ a contrastive objective that enforces the intra-view representation of the positive samples and can be distinguished from the inter-view representations of the negative samples. The contrastive objective is formulated as

follows:

$$\mathcal{L}_c = \underset{\omega, \phi, \psi}{\operatorname{argmax}} \sum_{i \in \mathcal{G}} \frac{1}{\tilde{C}(i)} \sum_{j \in C(i) \cap \{i\}} \hat{\mathcal{I}}_{\omega, \phi, \psi}(\mathbf{g}_j^\phi; \mathbf{d}_i^\psi) \quad (7)$$

where $\tilde{C}(i) := |C(i) + 1|$, $\hat{\mathcal{I}}_{\omega, \phi, \psi}$ is the mutual information estimator modeled by discriminator \mathcal{T}_ω and parameterized by a neural network with parameters ω . As stated in Hjelm et al. [12], contrastive learning-based methods concentrate primarily on the maximization of mutual information instead of its precise value. Therefore, we use the Jensen-Shannon MI estimator (following the formulation of [31]),

$$\begin{aligned} \hat{\mathcal{I}}_{\omega, \phi, \psi}(\mathbf{g}_j^\phi; \mathbf{d}_i^\psi) := & \mathbb{E}_{\mathbb{D}}[-sp(-\mathcal{T}_{\omega, \phi, \psi}(\mathbf{g}_j^\phi(\mathbf{x}); \mathbf{d}_i^\psi(\mathbf{x})))] \\ & - \mathbb{E}_{\mathbb{D} \times \tilde{\mathbb{D}}} [sp(\mathcal{T}_{\omega, \phi, \psi}(\mathbf{g}_j^\phi(\mathbf{x}'); \mathbf{d}_i^\psi(\mathbf{x})))] \end{aligned} \quad (8)$$

where x is an input sample, x' is an input sample from $\tilde{\mathbb{D}} = \mathbb{D}$, \mathbb{D} denotes an empirical probability distribution, and $sp(\cdot)$ is the softplus function. It should be noted that we generate negative samples using all possible combinations of inter/intra-view embeddings across all drugs in a batch. Since \mathbf{d}_i^ψ is encouraged to have high MI with samples containing information at both views, this favors encoding aspects of the data shared across different samples and views.

2.5 Drug-drug Interaction Prediction

2.5.1 Encoding Interaction Structural Information. According to the discussion in subsection 2.4, inspired by Zhang and Chen [52], before making predictions, we encode the substructure of each interaction for supplementary by using a Double-Radius Node Labeling(DRNL) algorithm. The algorithm labels neighboring nodes in each interaction's enclosing subgraph, which describes the " k -hop surrounding environment" around a given interaction based on the relative distance to the link. The intuition is that different nodes with different positions in the enclosing subgraph may play different roles during interaction prediction. Specifically, if we refer to the center nodes between the target interaction as a and b , nodes with different relative positions to the center nodes have different structural importance.

Formally, the DRNL algorithm can be described as follows:

$$\hat{D} = D(u, a) + D(u, b) \quad (9)$$

$$\begin{aligned} L(u) = & 1 + \min(D(u, a), D(u, b)) \\ & + \lfloor \hat{D}/2 \rfloor [\lfloor \hat{D}/2 \rfloor + (\hat{D} \bmod 2) - 1] \end{aligned} \quad (10)$$

where u denotes the node to be labeled in the enclosing subgraph, $D(p, q)$ is the shortest path distance between p and q , and $L(u)$ represents the label of u . For nodes that are not included in the enclosing subgraph or with $D(u, a) = \infty$ or $D(u, b) = \infty$, we label them as 0. It should be noted that b is temporally removed when calculating $D(u, a)$ otherwise $D(u, a)$ will be upper bounded by $D(u, b) + D(a, b)$. After obtaining neighboring nodes' labels, we concatenate them to generalize an interaction structural information vector $\mathbf{s} \in \mathbb{R}^n$. It is worth mentioning that the magnitude information in neighboring nodes' labels will be lost after one-hot encoding. That is why we directly use original labels.

2.5.2 Interaction predictor. For each interaction link $l_{ij} \in \mathcal{L}$, We first compress two drug embedding vectors into an interaction link embedding vector:

$$\mathbf{l} = \mathbf{d}_i \odot \mathbf{d}_j \quad (11)$$

where \odot denotes the element-wise product, \mathbf{l} is the interaction link embedding vector. Then, we concatenate \mathbf{l} and its corresponding structural information vector \mathbf{s} as the input for interaction prediction. We apply a two-layer fully-connected neural network to make the final prediction:

$$\mathbf{p} = \sigma(\mathbf{W}_p \operatorname{ReLU}(\mathbf{W}_l[\mathbf{l}; \mathbf{s}] + \mathbf{b}_l) + \mathbf{b}_p) \quad (12)$$

where $\mathbf{p} \in \mathbb{R}^k$ and $[\cdot; \cdot]$ denotes the concatenation operation. If the aim is to predict the occurrence of DDIs, k is 2, while k equals to the total number of DDI types if our target is to predict the specific DDI type(s).

Besides, we design another auxiliary interaction predictor using the inter-view drug embeddings. We cascade the last layer of the MPN with a fully connected layer and a sigmoid transformation function to construct this classifier. The prediction of the inter-view interaction predictor is denoted as $\mathbf{r} \in \mathbb{R}^k$. Optimizing the inter-view interaction prediction results can help the supervised information directly flow into previous network layers. The model learns the commonality between different views through a disagreement loss, which will be discussed below. So, finally, we get two prediction results corresponding to two different predictors. It should be noted that we only use \mathbf{p} for the final DDI prediction.

2.5.3 Training. Both predictors' primary goal is to minimize the supervised loss, which measures the distance between the predictions and the true labels. Another goal is to minimize a disagreement loss, which measures the distance between two predictors' predictions. The purpose of minimizing this disagreement loss is to enforce the model to pay more attention to the commonality between two different views and consistency between two predictors.

Formally, we formulate the supervised loss for the labeled interaction links and the disagreement loss for the unlabeled interaction links:

$$\mathcal{L}_s = \underset{\phi, \psi}{\operatorname{argmin}} \sum_{l_i \in \mathcal{L}_l} (\mathcal{E}(\mathbf{r}_i, y_i) + \mathcal{E}(\mathbf{p}_i, y_i)) \quad (13)$$

$$\mathcal{L}_d = \underset{\phi, \psi}{\operatorname{argmin}} \sum_{l_j \in \mathcal{L}_u} \mathcal{K}(\mathbf{p}_j || \mathbf{r}_j) \quad (14)$$

where y_i is the true label of l_i , \mathcal{L}_l and \mathcal{L}_u denote the labeled and unlabeled links in \mathcal{L} respectively, $\mathcal{E}(\cdot, \cdot)$ is the cross-entropy loss function and $\mathcal{K}(\cdot || \cdot)$ is the Kullback-Leibler divergence.

With contrastive loss \mathcal{L}_c , supervised loss \mathcal{L}_s and disagreement loss \mathcal{L}_d , the objective function of our model is,

$$\mathcal{L} = \mathcal{L}_s + \alpha \mathcal{L}_c + \beta \mathcal{L}_d \quad (15)$$

where α and β are hyper-parameters for the trade-off for different loss components. With the objective function, we use the back-propagation algorithm to find the best solution for the trainable parameters ω, ϕ, ψ .

3 EXPERIMENTS

In this section, we first describe the datasets, compared methods, and evaluation metrics used in the experiments. Then, we compare the proposed MIRACLE with other comparative methods. Finally, we make detailed analysis of MIRACLE under different experimental settings.

3.1 Datasets

We evaluate the proposed method on three benchmark datasets, i.e., *ZhangDDI*¹, *ChCh-Miner*² and *DeepDDI*³ with different scales for verifying the scalability and robustness of our model. These three datasets are small-scale, medium-scale, and large-scale, respectively. The *ZhangDDI* dataset contains a relatively small number of drugs where all the fingerprints are available for all drugs. However, for *DeepDDI*, the large-scale one, many fingerprints are missing in most drugs. For the *ChCh-Miner* dataset, although it has almost three times the number of drugs in the *ZhangDDI* dataset, it only has the same number of labeled DDI links. The statistics of datasets are summarized as follows:

- *ZhangDDI*[55]: This dataset contains 548 drugs and 48,548 pairwise DDIs and multiple types of similarity information about these drug pairs. We remove the data items that cannot be converted into graphs from SMILES strings in our preprocessing.
- *ChCh-Miner*[30]: This dataset contains 1,514 drugs and 48,514 DDI links without similarity-based fingerprints and polypharmacy side-effect information of each drug pair. We remove the data items that cannot be converted into graphs from SMILES strings in our preprocessing.
- *DeepDDI*[36]: This dataset contains 192,284 DDIs from 191,878 drug pairs and their polypharmacy side-effect information extracted from DrugBank[47]. We also remove the data items that cannot be converted into graphs from SMILES strings in our preprocessing.

3.2 Comparing Methods

To demonstrate the superiority of our proposed model, we implement many baseline approaches to compare their performance. The compared baselines cover similarity-based methods and graph-based methods. For the latter, to compare methods using different views of information reasonably, we define them under the same architecture as MIRACLE, which is summarized in table 1 and detailed as follows:

- **Nearest Neighbor**[45]: Vilar and his team used known interactions between drugs and similarity derived from substructure to conduct DDI prediction. We refer to the model as **NN** for simplicity.
- **Label Propagation**: Zhang et al. [54] utilized the label propagation(LP) algorithm to build three similarity-based predictive models. The similarity is calculated based on the substructure, side effect, and off-label side effect, respectively. We refer to the three models as **LP-Sub**, **LP-SE** and **LP-OSE**, respectively.

- **Multi-Feature Ensemble**: Zhang et al. [55] employed neighbor recommendation(NR) algorithm, label propagation(LP) algorithm, and matrix disturbs (MD) algorithm to build a hybrid ensemble model. The ensemble model exploited different aspects of drugs. We name the model as **Ens**.
- **SSP-MLP**: Ryu et al. [36] applied the combination of pre-computed low dimensional Structural Similarity Profile(SSP) and Multi-layer Perceptron to conduct the classification. We will refer to the model as **SSP-MLP**.
- **GCN**: Kipf and Welling [18] used a graph convolutional network(GCN) for semi-supervised node classification tasks. We applied **GCN** to encode drug molecular graphs and learn their representations to make predictions as a baseline.
- **GIN**: Xu et al. [49] proposed a graph isomorphism network (GIN) to learn molecules' representations in various single-body property prediction tasks. We used **GIN** to encode drug molecular graphs and learn their representations to make predictions as a baseline.
- **Attentive Graph Autoencoder**: Ma et al. [27] designed an attentive mechanism to integrate multiple drug similarity views, which will be fed into a graph autoencoder to learn the embedding vector for each drug. We referred to the model as **AttGA** and made predictions based on the learned drug representations pairwise as a baseline.
- **GAT**: Veličković et al. [43] utilized a graph attention network(GAT) to learn node embeddings by a well-designed attention mechanism on the graph. We used **GAT** to obtain drug embeddings on the DDI network for link prediction tasks.
- **SEAL-CI**: Li et al. [22] firstly applied a hierarchical graph representation learning framework in semi-supervised graph classification tasks. We named this model as **SEAL-CI** and used the model to learn drug representations for DDI link prediction as a baseline.
- **NFP-GCN**: Duvenaud et al. [6] is the first graph convolution operator, which is specific to molecules. We named the model as **NFP-GCN**. We changed our bond-aware message passing network into NFP to be a baseline.

3.3 Evaluation Metrics and Experimental Settings

We divide the entire interaction samples into a training set and a test set with a ratio of 4 : 1, and randomly select 1/4 of the training dataset as a validation dataset. Note that we have only reliable positive drug pairs in the dataset. We regard the same number of sampled negative drug pairs as the negative training samples for simplicity[3]. As for the test dataset, we let it be the same as the actual situation to preserve data imbalance by keeping the same distribution, whose numbers of positive samples to negative samples is about 1 : 2.

We set each parameter group's learning rate using an exponentially decaying schedule with the initial learning rate 0.0001 and multiplicative factor 0.96. For the proposed model's hyper-parameters, we set the dimension of the hidden state of atoms and drugs as 256. The total number of the bond-aware message passing neural networks and the GCN encoder is 3. The coefficients α and

¹<https://github.com/zw9977129/drug-drug-interaction/tree/master/dataset>

²<http://snap.stanford.edu/biodata/datasets/10001/10001-ChCh-Miner.html>

³<https://zenodo.org/record/1205795>

Table 1: Comparison of baseline methods.

Algorithm	Model Type	The Inter-view Model	The Intra-view Model	Feature Type
NN	similarity-based	N/A	N/A	similarity-based fingerprint
LP	similarity-based	N/A	N/A	similarity-based fingerprint
Ens	similarity-based	N/A	N/A	similarity-based fingerprint
SSP-MLP	similarity-based	N/A	N/A	similarity-based fingerprint
GCN	inter-view	GCN	N/A	Molecular Graph
GIN	inter-view	GIN	N/A	Molecular Graph
AttGA	intra-view	N/A	AttGA	Interaction Relationship
GAT	intra-view	N/A	GAT	Interaction Relationship
SEAL-CI	multi-view	GCN	GCN	Molecular Graph & Interaction Relationship
NFP-GCN	multi-view	NFP	GCN	Molecular Graph & Interaction Relationship
MIRACLE	multi-view	BAMPN	GCN	Molecular Graph & Interaction Relationship

β in objective functions are set to 100 and 0.8, respectively, making the model achieve the best performance. To further regularise the model, dropout[38] with $p = 0.3$ is applied to every intermediate layer’s output.

We implement our proposed model with Pytorch 1.4.0[33] and Pytorch-geometric 1.4.2[7]. Models are trained using Adam[17] optimizer. The model is initialized using Xavier[10] initialization. We choose three metrics to evaluate our proposed model’s effectiveness: *area under the ROC curve(AUROC)*, *area under the PRC curve(AUPRC)*, and *F1*. For multi-label classification, we choose the *macro* averages. We report the mean and standard deviation of these metrics over ten repetitions.

3.4 Experimental Results

We conduct experiments on three datasets with different characteristics to verify our proposed method’s effectiveness in different scenarios. The three parts of the experiments validate the superiority of our MIRACLE method compared to baselines on the small scale dataset with all types of drug features and the medium scale dataset with few labeled DDI links for the binary classification task, and the large scale dataset with missing drug features for the multi-label classification task, respectively.

3.4.1 Comparison on the ZhangDDI dataset. Table 2 compares our MIRACLE model’s performance against baseline approaches on the *ZhangDDI* dataset, where almost all types of drug features can be used for the DDI prediction task. The best results are highlighted in boldface. MIRACLE integrates multi-view information into drug representations. In this model, we jointly consider the inter-view drug molecular graphs and the intra-view DDI relationships. According to the experiments, the proposed model achieves more excellent performance compared to these baseline approaches.

The performance of algorithms utilizing similarity-based fingerprints like **NN**, **LP**, and **SSP-MLP** is relatively poor, which only incorporate one kind of very important features. However, contrary to them, **Ens** obtains better results because of the combination of three distinct models utilizing eight types of drug feature similarities coupling with another six types of topological ones, demonstrating the importance of integrating information from multiple sources like similarity-based fingerprints and topological features.

Some graph-based methods perform worse than the models mentioned above because they only rely on the single view graph information. **GCN** and **GIN** encode drug molecular graphs by two different graph neural network frameworks. They make DDI predictions pairwise based on the obtained drug molecule representations. **AttGA** and **GAT** directly learn drug representations from DDI interaction relationships and make predictions using the inner product results of target drug pairs’ embeddings. The former acquires multiple connectivities of the DDI network according to different similarity matrices and applies a GCN encoder to obtain drug representations with varying relationships of interaction. This method fuses these drug representations to make final predictions that distinctly can achieve better performance than **GAT**, who only considers the DDI network’s link existence.

The compared baselines in the multi-view graph settings like **SEAL-CI** and **NFP-GCN** outperform other baselines, demonstrating the integration of multi-view graph can improve the performance of models significantly. However, their performance is still inferior to that of the proposed method. Compared with the state-of-art method, MIRACLE further considers the importance of the message passing mechanism in terms of chemical bonds inside drug molecular graphs and the balance between multi-view graph information, which can learn more comprehensive drug representations. Whereas in **SEAL-CI** and **NFP-GCN**, they explicitly model the multi-view graphs and obtain the drug representations through a continuous graph neural network pipeline, with information equilibrium between different views ignored. Besides, **MIRACLE** adopts the self-attentive mechanism to generate an inter-view drug representation that automatically selects the most significant atoms that form meaningful functional groups in DDI reactions and neglect noisy, meaningless substructures.

3.4.2 Comparison on the ChCh-Miner dataset. In this part of the experiment, we aim to evaluate our proposed **MIRACLE** method on datasets with few labeled DDI links. We only compare **MIRACLE** with graph-based baselines because this dataset lacks similarity-based fingerprints for drug pairs. For the same reason, **AttGA** does not apply to this dataset. Table 3 shows the results.

Obviously, methods taking multi-view information into consideration like **SEAL-CI** and **NFP-GCN** outperform baselines who only use single-view information. However, **MIRACLE** achieves

Table 2: Comparative evaluation results on *ZhangDDI*

Algorithm	Performance		
	AUROC	AUPRC	F1
NN	67.81 ± 0.25	52.61 ± 0.27	49.84 ± 0.43
LP-Sub	93.39 ± 0.13	89.15 ± 0.13	79.61 ± 0.16
LP-SE	93.48 ± 0.25	89.61 ± 0.19	79.83 ± 0.61
LP-OSE	93.50 ± 0.24	90.31 ± 0.82	80.41 ± 0.51
Ens	95.20 ± 0.14	92.51 ± 0.15	85.41 ± 0.16
SSP-MLP	92.51 ± 0.15	88.51 ± 0.66	80.69 ± 0.81
GCN	91.91 ± 0.62	88.73 ± 0.84	81.61 ± 0.39
GIN	81.45 ± 0.26	77.16 ± 0.16	64.15 ± 0.16
AttGA	92.84 ± 0.61	90.21 ± 0.19	70.96 ± 0.39
GAT	91.49 ± 0.29	90.69 ± 0.10	80.93 ± 0.25
SEAL-CI	92.93 ± 0.19	92.82 ± 0.17	84.74 ± 0.17
NFP-GCN	93.22 ± 0.09	93.07 ± 0.46	85.29 ± 0.38
MIRACLE	98.95 ± 0.15	98.17 ± 0.06	93.20 ± 0.27

Table 3: Comparative evaluation results on *ChCh-Miner*

Algorithm	Performance		
	AUROC	AUPRC	F1
GCN	82.84 ± 0.61	84.27 ± 0.66	70.54 ± 0.87
GIN	70.32 ± 0.87	72.41 ± 0.63	65.54 ± 0.97
GAT	85.84 ± 0.23	88.14 ± 0.25	76.51 ± 0.38
SEAL-CI	90.93 ± 0.19	89.38 ± 0.39	84.74 ± 0.48
NFP-GCN	92.12 ± 0.09	93.07 ± 0.69	85.41 ± 0.18
MIRACLE	96.15 ± 0.29	95.57 ± 0.19	92.26 ± 0.09

the best performance and substantially exceeds baselines, demonstrating the superiority of our proposed method on datasets with few labeled data.

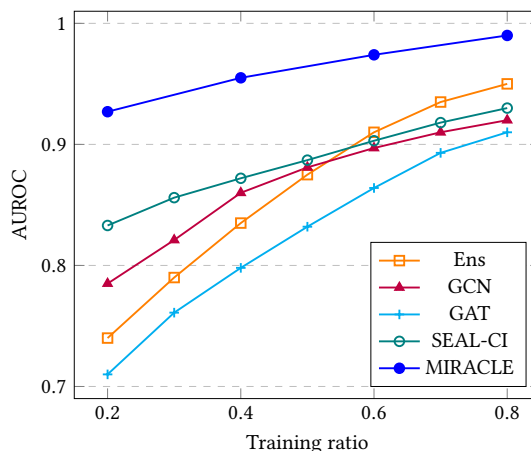
The graph contrastive learning component integrates and balances information from different views, **MIRACLE** learns drug representations better with less labeled DDI links. The proposed method also considers the DDI network’s structural information when making the final predicting decisions, which helps the model extracts the most useful information from all dimensional features for DDI prediction. We further verify our points by a small ablation study in which we adjust the training ratio of the dataset in subsection 3.5.

3.4.3 Comparison on the DeepDDI dataset. To verify our proposed method’s scalability, we also conduct experiments on a large-scale dataset, *DeepDDI*, which has plenty of labeled data and multiple types of DDI information. Table 4 compares our proposed approach’s performance to the baseline methods specially designed for the prediction of specific DDI type. Many baseline approaches utilizing similarity-based fingerprints need plenty of non-structural similarity features, which may be absent in this large scale dataset. Therefore, we only select models who are applicable in this dataset, including **NN** and **SSP-MLP**. For the graph-based methods, we neglect **AttGA** for the lack of many needed drug features. We also ignore experimental results obtained by **GIN** and **NFP-GCN** because of the worse performance and the space limitation.

Table 4: Comparative evaluation results on *DeepDDI*

Algorithm	Performance		
	AUROC	AUPRC	F1
NN	81.81 ± 0.37	80.82 ± 0.20	71.37 ± 0.18
SSP-MLP	92.28 ± 0.18	90.27 ± 0.28	79.71 ± 0.16
GCN	85.53 ± 0.17	83.27 ± 0.31	72.18 ± 0.22
GAT	84.84 ± 0.23	81.14 ± 0.25	73.51 ± 0.38
SEAL-CI	92.83 ± 0.19	90.44 ± 0.39	80.70 ± 0.48
MIRACLE	95.51 ± 0.27	92.34 ± 0.17	83.60 ± 0.33

MLP-SSP substantially outperforms **NN** for the former framework is based on deep neural networks. **GCN** achieves better performance than **GAT**, which further demonstrates the inter-view information plays a vital role in DDI predictions. **SEAL-CI** is second to the proposed method among the baselines proving the superiority of the multi-view graph framework. **MIRACLE** significantly outperformed other baseline methods in terms of all the three metrics.

**Figure 4: Results of the compared methods on *ZhangDDI* with different training ratio**

3.5 Ablation Study

We conduct ablation experiments on the *ZhangDDI* and the *ChCh-Miner* dataset to validate the contrastive learning component’s effectiveness in our model. The experimental results are reported in table 5. To better understand the differences between **MIRACLE** with and without the contrastive learning component, we visualize their drug embeddings using the visualization tool t-SNE[29], which projects each method’s learned embeddings in a 2D space. Figure 6 shows the results on the *ChCh-Miner* dataset. From the figure, we can observe that **MIRACLE** effectively learns drug embeddings with the contrastive learning component. We also analyze our proposed method’s robustness with a different number of labeled training data by adjusting the training set ratio on the *ZhangDDI* dataset. As seen in figure 4, **MIRACLE** with the contrastive learning component

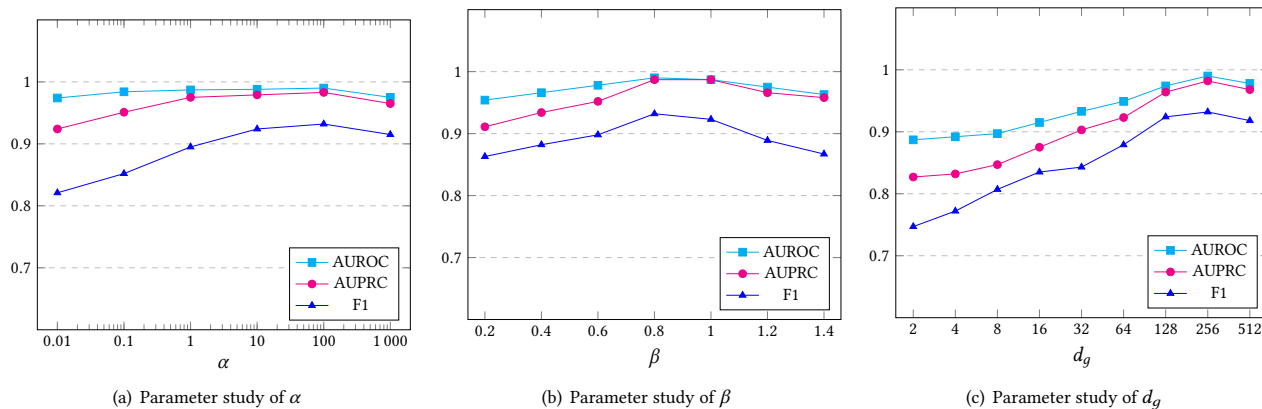
Figure 5: Parameter sensitivity study on *ZhangDDI*

Table 5: Ablation experimental results

Dataset	Algorithm	Performance		
		AUROC	AUPRC	F1
ZhangDDI	-C	96.62 \pm 0.17	92.15 \pm 0.31	89.42 \pm 0.22
	MIRACLE	98.95 \pm 0.15	98.17 \pm 0.06	93.20 \pm 0.27
ChCh-Miner	-C	93.37 \pm 0.40	94.84 \pm 0.38	90.38 \pm 0.15
	MIRACLE	96.15 \pm 0.29	95.57 \pm 0.19	92.26 \pm 0.09

can also achieve high performance, validating its superiority in the scenario with few labeled data.

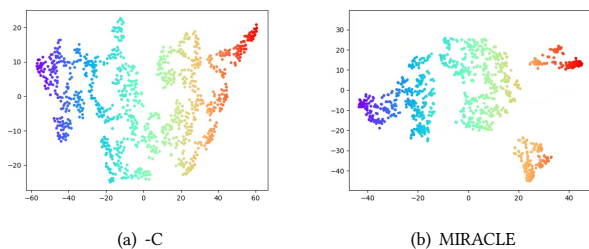


Figure 6: Visualization of drug embeddings on *ChCh-Miner*. (The drug embeddings visualized in the left picture is learned by MIRACLE without the contrastive learning component, and those in the right one is learned directly by MIRACLE.)

3.6 Parameter Sensitivity

In our model in equation 15, there are two major parameters α and β . In this subsection, we evaluate the impacts of them, together with the dimensionality of drug embeddings d_g on the *ZhangDDI* dataset. Figure 5(a) and 5(b) show the results by changing one parameter while fixing another one.

First, we vary α by $\{0.01, 0.1, 1, 10, 100, 1000\}$, and fix $\beta = 0.8$, $d_g = 256$. Here, for parameter study purpose, β is set to its optimal value on this dataset instead of the default value 1. From the figure,

our method is quite stable in a wide range of α and achieves the best performance when $\alpha = 100$ in terms of *AUROC*. Next, we vary β by $\{0.2, 0.4, 0.6, 0.8, 1, 1.2, 1.4\}$ with $\alpha = 100$ and $d_g = 256$. As can be seen, the near optimal performance at $\beta = 0.8$ justifies our parameter setting. Overall, α and β are stable w.r.t these parameters. Moreover, the non-zero choices of α and β demonstrate the importance of the loss terms in our model.

To evaluate d_g , we vary it from 2 to 512, and fix $\alpha = 10$ and $\beta = 0.8$. The results are shown in figure 5(c). From the figure, MIRACLE is robust to d_g . Specifically, when d_g is small, the *AUROC* increases because higher dimensionality can encode more useful information. When d_g reaches its optimal value, the accuracy begins to drop slightly because a too high dimensionality may introduce redundant and noisy information that can harm the classification performance.

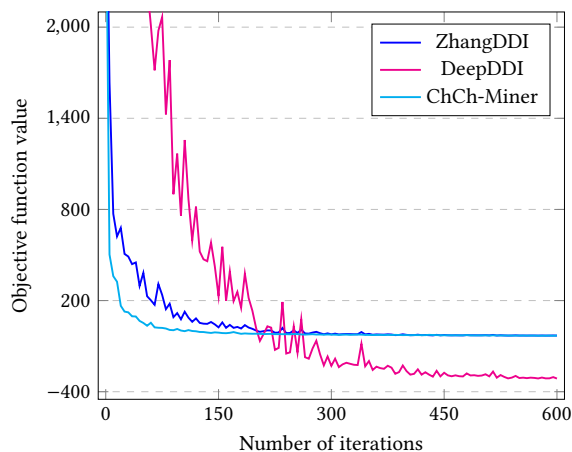


Figure 7: Convergence evaluation

3.7 Convergence Evaluation

In this subsection, we study the proposed MIRACLE algorithm’s performance in terms of the number of iterations before converging to a local optimum. Figure 7 shows the value of the objective function \mathcal{L} in equation 15 with respect to the number of iterations on different datasets. From the figure, we observe the objective function value decreases steadily with more iterations. Usually, less than 600 iterations are sufficient for convergence.

4 RELATED WORK

DDI prediction. There is little doubt that the most accurate way for predicting DDIs is *in vivo* or *in vitro* trials. But such bioassay is practicable only on a small set of drugs and limited by the experimental environment[5]. With the accumulation of biomedical data, many machine learning methods are proposed for DDI prediction. To the best of our knowledge, most existing DDI prediction methods could be divided into feature-based and graph-based.

The feature-based methods adopt the assumption: **drugs sharing similar chemical structures are prone to share similar DDIs**. Vilar et al. [45, 46] generate DDI candidates by comparing the Tanimoto coefficient between human-curated fingerprint vectors of drugs. Celebi et al. [2] employs a rooted page rank algorithm that integrates therapeutic, genomic, phenotypic, and chemical similarity to discover novel DDIs. Zhang et al. [54] proposes a label propagation framework considering immediate structure similarity from PubChem and high-order similarity from divergent clinical databases. Huang et al. [13], Luo et al. [26] measure the connections between drugs and targets to predict pharmacodynamic DDIs, which could be regarded as another aspect of drug similarity. Ryu et al. [36] proposes DeepDDI, which applies a feed-forward neural network to encode structural similarity profile (SSP) of drugs to predict DDI. Although similarity-based methods yield robust results on DDI prediction tasks, these methods may have limitations on digging novel DDIs, i.e., not scalable. Starting with known drug interactions, it is far from sufficient to use similarity criteria to model complex DDIs, let alone the number of DDIs identified is still sparse. For high-hanging fruits, more prior knowledge and higher-level representations are required for novel DDI detection.

The factor mentioned above pushes the community to focus on feature-based methods. Besides features from drugs, feature-based methods usually include other prior information, such as chemical properties and biological regulation.

Recently, graph-based methods like neural fingerprint[6], message passing network[9] and graph representation learning[11] have proved to be successful on molecular tasks, several graph neural networks (GNNs) are proved to have a good DDI prediction power. Zhang et al. [54, 55] make DDI predictions based on nearest neighbors, though these works learn representations from multiple prior information, but failed to take relations of DDIs into account, such as transitivity of similarities. Ma et al. [28] uses attentive graph auto-encoders[19] to integrates heterogeneous information from divergent drug-related data sources. Decagon[58] introduces another graph auto-encoder, making an end-to-end generation of link prediction predictions in the drug-protein network. This work shows that deep GNNs outperform traditional shallow architectures significantly, such as static fingerprints[6], DeepDDI[36], and

traditional graph embedding methods[34, 59]. More recently, Lin et al. [25] merges several datasets into a vast knowledge graph with 1.2 billion triples. Through KGNN layers which embed 2-hop local structures of drugs, this model outperforms both graph embedding based methods such as random walk[34], struct2vec[35], LINE[41] and deep learning-based methods such as DeepDDI[36] plus same knowledge graph-based method KG-ddi[14]. With the help of such graph models, higher-level representations are learned from a variety of graph-structured data.

Neural network for graphs. Graph neural networks extend the convolutional neural network to non-Euclidean spaces, providing a more natural and effective way for modeling graph-structured data[9]. In recent years, numerous powerful GNN architectures are reported[1, 6, 11, 16, 18, 24, 37, 43, 49, 50, 53]. With the development of various GNNs and variants, modern GNNs have achieved state-of-the-art performances in link prediction, node classification, graph classification. Generally, a typical GNN follows a three-step message passing scheme to generate node or graph level representation. 1) Aggregate step integrates neighbor embeddings which serve as messages; 2) combine step update the representation of nodes based on messages in 1); 3) readout step is a permutation invariant function that produces graph-level representation from node-level representations. In each layer of GNN, node features are updated by its immediate neighbors. Thus, after k iterations (layers), a node’s embedding vector encodes the k -hop subgraph’s topological features. Finally, a graph-level embedding reflecting overall structure could be computed by readout function if needed.

Recently, contrastive learning revitalizes in many fields, and graph representation learning is no exception. Inspired by previous success in visual representation learning, Veličković et al. [44] proposes a MI maximization objective to maximize the MI between node embeddings and the graph embedding by discriminating nodes in the original graph from nodes in a corrupted graph. Sun et al. [40] extends the MI maximization objective to better learn the graph-level representation by maximizing the MI between the graph-level representation and the representations of substructures of different scales. Zhu et al. [56] proposes a new method to generate different graph views by removing edges and masking features and maximizing the agreement of node embeddings between two graph views. Inspired by the information maximization principle, we apply the MI maximization objective in balancing information from different views in drug embeddings.

5 CONCLUSION

To better integrate the rich multi-view graph information in the DDI network, we propose MIRACLE for the DDI prediction task in this paper. MIRACLE learns drug embeddings from a multi-view graph perspective by designing an end-to-end framework that consists of a bond-aware message passing network and a GCN encoder. Then, a novel contrastive learning-based strategy has been proposed to balance information from different views. Also, we design two predictors from both views to fully exploit the available information. Through extensive experiments on various real-life datasets, we have demonstrated that the proposed MIRACLE is both effective and efficient.

REFERENCES

- [1] Peter Battaglia, Razvan Pascanu, Matthew Lai, Danilo Jimenez Rezende, et al. 2016. Interaction networks for learning about objects, relations and physics. In *Advances in neural information processing systems*. 4502–4510.
- [2] Remzi Celebi, Vahab Mostafapour, Erkan Yasar, Özgür Gümüş, and Oguz Dikenelli. 2015. Prediction of Drug-Drug interactions using pharmacological similarities of drugs. In *2015 26th International Workshop on Database and Expert Systems Applications (DEXA)*. IEEE, 14–17.
- [3] Xin Chen, Xien Liu, and Ji Wu. 2019. Drug-drug Interaction Prediction with Graph Representation Learning. In *2019 IEEE International Conference on Bioinformatics and Biomedicine (BIBM)*. IEEE, 354–361.
- [4] Andreea Deac, Yu-Hsiang Huang, Petar Veličković, Pietro Liò, and Jian Tang. 2019. Drug-drug adverse effect prediction with graph co-attention. *arXiv preprint arXiv:1905.00534* (2019).
- [5] Jon D Duke, Xu Han, Zhiping Wang, Abhinata Subhadarshini, Shreyas D Karnik, Xiaochun Li, Stephen D Hall, Yan Jin, J Thomas Callaghan, Marcus J Overhage, et al. 2012. Literature based drug interaction prediction with clinical assessment using electronic medical records: novel myopathy associated drug interactions. *PLoS Comput Biol* 8, 8 (2012), e1002614.
- [6] David K Duvenaud, Dougal Maclaurin, Jorge Iparraguirre, Rafael Bombarell, Timothy Hirzel, Alan Aspuru-Guzik, and Ryan P Adams. 2015. Convolutional networks on graphs for learning molecular fingerprints. In *Advances in neural information processing systems*. 2224–2232.
- [7] Matthias Fey and Jan Eric Lenssen. 2019. Fast graph representation learning with PyTorch Geometric. *arXiv preprint arXiv:1903.02428* (2019).
- [8] Justin Gilmer, Samuel S Schoenholz, Patrick F Riley, Oriol Vinyals, and George E Dahl. 2017. Neural message passing for quantum chemistry. *arXiv preprint arXiv:1704.01212* (2017).
- [9] Justin Gilmer, Samuel S. Schoenholz, Patrick F. Riley, Oriol Vinyals, and George E. Dahl. 2017. Neural Message Passing for Quantum Chemistry. In *Proceedings of the 34th International Conference on Machine Learning, ICML 2017, Sydney, NSW, Australia, 6–11 August 2017 (Proceedings of Machine Learning Research)*, Doina Precup and Yee Whye Teh (Eds.), Vol. 70. PMLR, 1263–1272. <http://proceedings.mlr.press/v70/gilmer17a.html>
- [10] Xavier Glorot and Yoshua Bengio. 2010. Understanding the difficulty of training deep feedforward neural networks. In *Proceedings of the thirteenth international conference on artificial intelligence and statistics*. 249–256.
- [11] Will Hamilton, Zhitao Ying, and Jure Leskovec. 2017. Inductive representation learning on large graphs. In *Advances in neural information processing systems*. 1024–1034.
- [12] R Devon Hjelm, Alex Fedorov, Samuel Lavoie-Marchildon, Karan Grewal, Phil Bachman, Adam Trischler, and Yoshua Bengio. 2018. Learning deep representations by mutual information estimation and maximization. *arXiv preprint arXiv:1808.06670* (2018).
- [13] Jialiang Huang, Chaoqun Niu, Christopher D Green, Lun Yang, Hongkang Mei, and Jing-Dong J Han. 2013. Systematic prediction of pharmacodynamic drug-drug interactions through protein-protein-interaction network. *PLoS Comput Biol* 9, 3 (2013), e1002998.
- [14] Md Rezaul Karim, Michael Cochez, Joao Bosco Jares, Mamta Uddin, Oya Beyan, and Stefan Decker. 2019. Drug-drug interaction prediction based on knowledge graph embeddings and convolutional-LSTM network. In *Proceedings of the 10th ACM International Conference on Bioinformatics, Computational Biology and Health Informatics*. 113–123.
- [15] Andrej Kastrin, Polonca Ferik, and Brane Leskošek. 2018. Predicting potential drug-drug interactions on topological and semantic similarity features using statistical learning. *PLOS ONE* 13, 5 (05 2018), 1–23. <https://doi.org/10.1371/journal.pone.0196865>
- [16] Steven Kearnes, Kevin McCloskey, Marc Berndl, Vijay Pande, and Patrick Riley. 2016. Molecular graph convolutions: moving beyond fingerprints. *Journal of computer-aided molecular design* 30, 8 (2016), 595–608.
- [17] Diederik P Kingma and Jimmy Ba. 2014. Adam: A method for stochastic optimization. *arXiv preprint arXiv:1412.6980* (2014).
- [18] Thomas N Kipf and Max Welling. 2016. Semi-supervised classification with graph convolutional networks. *arXiv preprint arXiv:1609.02907* (2016).
- [19] Thomas N Kipf and Max Welling. 2016. Variational graph auto-encoders. *arXiv preprint arXiv:1611.07308* (2016).
- [20] Greg Landrum. 2013. RDKit: A software suite for cheminformatics, computational chemistry, and predictive modeling.
- [21] Jason Lazarou, Bruce H Pomeranz, and Paul N Corey. 1998. Incidence of adverse drug reactions in hospitalized patients: a meta-analysis of prospective studies. *Jama* 279, 15 (1998), 1200–1205.
- [22] Jia Li, Yu Rong, Hong Cheng, Helen Meng, Wenbing Huang, and Junzhou Huang. 2019. Semi-supervised graph classification: A hierarchical graph perspective. In *The World Wide Web Conference*. 972–982.
- [23] Qimai Li, Zhichao Han, and Xiao-Ming Wu. 2018. Deeper insights into graph convolutional networks for semi-supervised learning. *arXiv preprint arXiv:1801.07606* (2018).
- [24] Yujia Li, Daniel Tarlow, Marc Brockschmidt, and Richard Zemel. 2015. Gated graph sequence neural networks. *arXiv preprint arXiv:1511.05493* (2015).
- [25] Xuan Lin, Zhe Quan, Zhi-Jie Wang, Tengfei Ma, and Xiangxiang Zeng. 2020. Kgnn: Knowledge graph neural network for drug-drug interaction prediction. *IJCAI*.
- [26] Heng Luo, Ping Zhang, Hui Huang, Jialiang Huang, Emily Kao, Leming Shi, Lin He, and Lun Yang. 2014. DDI-CPI, a server that predicts drug-drug interactions through implementing the chemical-protein interactome. *Nucleic acids research* 42, W1 (2014), W46–W52.
- [27] Tengfei Ma, Cao Xiao, Jiayu Zhou, and Fei Wang. 2018. Drug similarity integration through attentive multi-view graph auto-encoders. *arXiv preprint arXiv:1804.10850* (2018).
- [28] Tengfei Ma, Cao Xiao, Jiayu Zhou, and Fei Wang. 2018. Drug Similarity Integration through Attentive Multi-View Graph Auto-Encoders. In *Proceedings of the 27th International Joint Conference on Artificial Intelligence (IJCAI’18)*. AAAI Press, 3477–3483.
- [29] Laurens van der Maaten and Geoffrey Hinton. 2008. Visualizing data using t-SNE. *Journal of machine learning research* 9, Nov (2008), 2579–2605.
- [30] Sagar Maheshwari Marinka Zitnik, Rok Sosič and Jure Leskovec. 2018. BioSNAP Datasets: Stanford Biomedical Network Dataset Collection. <http://snap.stanford.edu/biodata>.
- [31] Sebastian Nowozin, Botond Cseke, and Ryota Tomioka. 2016. f-gan: Training generative neural samplers using variational divergence minimization. In *Advances in neural information processing systems*. 271–279.
- [32] Caterina Palleria, Antonello Di Paolo, Chiara Giofrè, Chiara Caglioti, Giacomo Leuzzi, Antonio Siniscalchi, Giovambattista De Sarro, and Luca Gallelli. 2013. Pharmacokinetic drug-drug interaction and their implication in clinical management. *Journal of research in medical sciences: the official journal of Isfahan University of Medical Sciences* 18, 7 (2013), 601.
- [33] Adam Paszke, Sam Gross, Francisco Massa, Adam Lerer, James Bradbury, Gregory Chanan, Trevor Killeen, Zeming Lin, Natalia Gimelshein, Luca Antiga, et al. 2019. Pytorch: An imperative style, high-performance deep learning library. In *Advances in neural information processing systems*. 8026–8037.
- [34] Bryan Perozzi, Rami Al-Rfou, and Steven Skiena. 2014. Deepwalk: Online learning of social representations. In *Proceedings of the 20th ACM SIGKDD international conference on Knowledge discovery and data mining*. 701–710.
- [35] Leonardo FR Ribeiro, Pedro HP Saverese, and Daniel R Figueiredo. 2017. struc2vec: Learning node representations from structural identity. In *Proceedings of the 23rd ACM SIGKDD international conference on knowledge discovery and data mining*. 385–394.
- [36] Jae Yong Ryu, Hyun Uk Kim, and Sang Yup Lee. 2018. Deep learning improves prediction of drug-drug and drug-food interactions. *Proceedings of the National Academy of Sciences* 115, 18 (2018), E4304–E4311.
- [37] Franco Scarselli, Marco Gori, Ah Chung Tsoi, Markus Hagenbuchner, and Gabriele Monfardini. 2008. The graph neural network model. *IEEE Transactions on Neural Networks* 20, 1 (2008), 61–80.
- [38] Nitish Srivastava, Geoffrey Hinton, Alex Krizhevsky, Ilya Sutskever, and Ruslan Salakhutdinov. 2014. Dropout: a simple way to prevent neural networks from overfitting. *The journal of machine learning research* 15, 1 (2014), 1929–1958.
- [39] Rupesh Kumar Srivastava, Klaus Greff, and Jürgen Schmidhuber. 2015. Highway networks. *arXiv preprint arXiv:1505.00387* (2015).
- [40] Fan-Yun Sun, Jordan Hoffmann, Vikas Verma, and Jian Tang. 2019. Infograph: Un-supervised and semi-supervised graph-level representation learning via mutual information maximization. *arXiv preprint arXiv:1908.01000* (2019).
- [41] Jian Tang, Meng Qu, Mingzhe Wang, Ming Zhang, Jun Yan, and Qiaozhu Mei. 2015. Line: Large-scale information network embedding. In *Proceedings of the 24th international conference on world wide web*. 1067–1077.
- [42] Ashish Vaswani, Noam Shazeer, Niki Parmar, Jakob Uszkoreit, Llion Jones, Aidan N Gomez, Łukasz Kaiser, and Illia Polosukhin. 2017. Attention is all you need. In *Advances in neural information processing systems*. 5998–6008.
- [43] Petar Veličković, Guillem Cucurull, Arantxa Casanova, Adriana Romero, Pietro Liò, and Yoshua Bengio. 2017. Graph attention networks. *arXiv preprint arXiv:1710.10903* (2017).
- [44] Petar Veličković, William Fedus, William L Hamilton, Pietro Liò, Yoshua Bengio, and R Devon Hjelm. 2018. Deep graph infomax. *arXiv preprint arXiv:1809.10341* (2018).
- [45] Santiago Vilar, Rave Harpaz, Eugenio Uriarte, Lourdes Santana, Raul Rabadan, and Carol Friedman. 2012. Drug-drug interaction through molecular structure similarity analysis. *Journal of the American Medical Association* 19, 6 (2012), 1066–1074.
- [46] Santiago Vilar, Eugenio Uriarte, Lourdes Santana, Tal Lorberbaum, George Hripsak, Carol Friedman, and Nicholas P Tatonetti. 2014. Similarity-based modeling in large-scale prediction of drug-drug interactions. *Nature protocols* 9, 9 (2014), 2147.
- [47] David S Wishart, Yannick D Feunang, An C Guo, Elvis J Lo, Ana Marcu, Jason R Grant, Tanvir Sajed, Daniel Johnson, Carin Li, Zinat Sayeeda, et al. 2018. DrugBank 5.0: a major update to the DrugBank database for 2018. *Nucleic acids research* 46, D1 (2018), D1074–D1082.

- [48] CHEN Xin, LIU Xien, and WU Ji. 2020. Research progress on drug representation learning. *Journal of Tsinghua University (Science and Technology)* 60, 2 (2020), 171–180.
- [49] Keyulu Xu, Weihua Hu, Jure Leskovec, and Stefanie Jegelka. 2018. How powerful are graph neural networks? *arXiv preprint arXiv:1810.00826* (2018).
- [50] Keyulu Xu, Chengtao Li, Yonglong Tian, Tomohiro Sonobe, Ken-ichi Kawarabayashi, and Stefanie Jegelka. 2018. Representation learning on graphs with jumping knowledge networks. *arXiv preprint arXiv:1806.03536* (2018).
- [51] Shuicheng Yan, Dong Xu, Benyu Zhang, Hong-Jiang Zhang, Qiang Yang, and Stephen Lin. 2006. Graph embedding and extensions: A general framework for dimensionality reduction. *IEEE transactions on pattern analysis and machine intelligence* 29, 1 (2006), 40–51.
- [52] Muhan Zhang and Yixin Chen. 2018. Link prediction based on graph neural networks. In *Advances in Neural Information Processing Systems*. 5165–5175.
- [53] Muhan Zhang, Zhicheng Cui, Marion Neumann, and Yixin Chen. 2018. An end-to-end deep learning architecture for graph classification. In *Thirty-Second AAAI Conference on Artificial Intelligence*.
- [54] Ping Zhang, Fei Wang, Jianying Hu, and Robert Sorrentino. 2015. Label propagation prediction of drug-drug interactions based on clinical side effects. *Scientific reports* 5, 1 (2015), 1–10.
- [55] Wen Zhang, Yanlin Chen, Feng Liu, Fei Luo, Gang Tian, and Xiaohong Li. 2017. Predicting potential drug-drug interactions by integrating chemical, biological, phenotypic and network data. *BMC bioinformatics* 18, 1 (2017), 18.
- [56] Yanqiao Zhu, Yichen Xu, Feng Yu, Qiang Liu, Shu Wu, and Liang Wang. 2020. Deep Graph Contrastive Representation Learning. *arXiv preprint arXiv:2006.04131* (2020).
- [57] Marinka Zitnik, Monica Agrawal, and Jure Leskovec. 2018. Modeling polypharmacy side effects with graph convolutional networks. *Bioinformatics* 34, 13 (2018), 457–466.
- [58] Marinka Zitnik, Monica Agrawal, and Jure Leskovec. 2018. Modeling polypharmacy side effects with graph convolutional networks. *Bioinformatics* 34, 13 (2018), i457–i466.
- [59] Nansu Zong, Hyeoneui Kim, Victoria Ngo, and Olivier Harismendy. 2017. Deep mining heterogeneous networks of biomedical linked data to predict novel drug–target associations. *Bioinformatics* 33, 15 (2017), 2337–2344.